

Supplementary information for:

Characterizing surface states in hematite nanorod photoanodes, both beneficial and detrimental to solar water splitting efficiency

Dana Stanescu^{a*}, Mekan Piriye^b, Victoria Villard^a, Cristian Mocuta^b, Adrien Besson^b, Dris Ihiawakrim^c, Ovidiu Ersen^c, Jocelyne Leroy^d, Sorin G. Chiuzbaian^e, Adam P. Hitchcock^f, Stefan Stanescu^{b*}

^a Service de Physique de l'Etat Condensé (SPEC), CEA, CNRS UMR 3680, Université Paris-Saclay, Orme des Merisiers, CEA Saclay, 91191 Gif-sur-Yvette Cedex, France, dana.stanescu@cea.fr

^b Synchrotron SOLEIL, L'Orme des Merisiers, Saint-Aubin, BP 48, 91192 Gif-sur-Yvette Cedex, France, stefan.stanescu@synchrotron-soleil.fr

^c Institut de Physique et Chimie des Matériaux de Strasbourg (IPCMS), UMR 7504 CNRS – Université de Strasbourg, 23 rue du Loess, BP 43, Strasbourg Cedex 2, France

^d Nanosciences et Innovation pour les Matériaux, la Biomédecine et l'Énergie (NIMBE), CEA, CNRS UMR 3685, Université Paris-Saclay, CEA Saclay, 91191 Gif-sur-Yvette Cedex, France

^e Sorbonne Universités, UPMC Univ. Paris 06, CNRS, Laboratoire de Chimie Physique – Matière et Rayonnement (UMR 7614), 4 place Jussieu, 75252 Paris Cedex 05, France

^f Chemistry & Chemical Biology, McMaster University Hamilton, ON, Canada

* Corresponding authors: dana.stanescu@cea.fr, stefan.stanescu@synchrotron-soleil.fr

Table SI-1: Growth parameters for pure and Ti-substituted hematite samples produced at pH = 1.4 and activation hydrothermal temperature of 95°C. The hydrothermal growth time was adjusted in order to obtain similar length (~200 nm) of the nanorods for all the samples.

Sample		ACG time (h)	Ti in FeCl ₃ (wt.%)	Annealing T (°C)
S1	α -Fe ₂ O ₃	4	0	500
S2		8		600
S3	Ti: α -Fe ₂ O ₃	23	0.3	500
S4		22		600

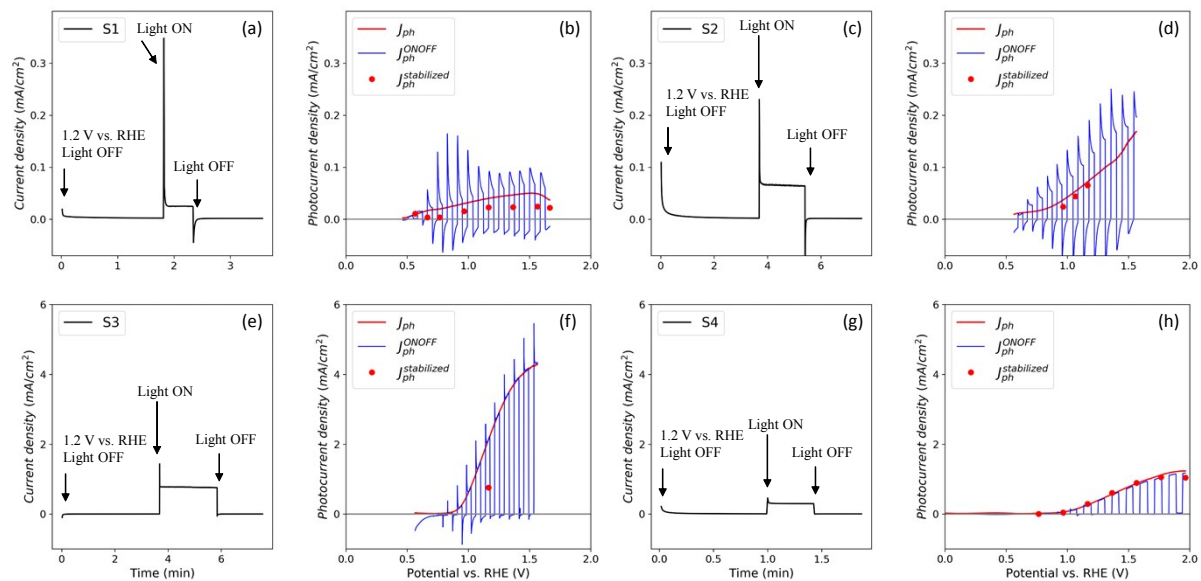


Figure SI-1: (a, c, e, g) Current density vs. time obtained on samples S1, S2, S3 and S4 respectively for $V = 1.2$ V vs. RHE. The time stabilized photocurrent values are obtained following the ON/OFF scheme indicated on the graphs. (b, d, f, h) fast sweep voltammetry photocurrent (red line) and ON-OFF (blue line) curves obtained for S1, S2, S3 and S4, respectively. The stabilized values of the photocurrent are indicated as red dots.

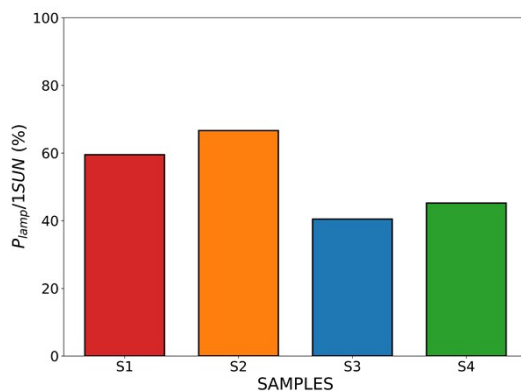


Figure SI-2: Integrated lamp power values obtained during the calibrations performed prior to each experimental PEC session. The reported values in the paper are normalized to these values assuming a linear dependence of the lamp power and the resulting photocurrent.

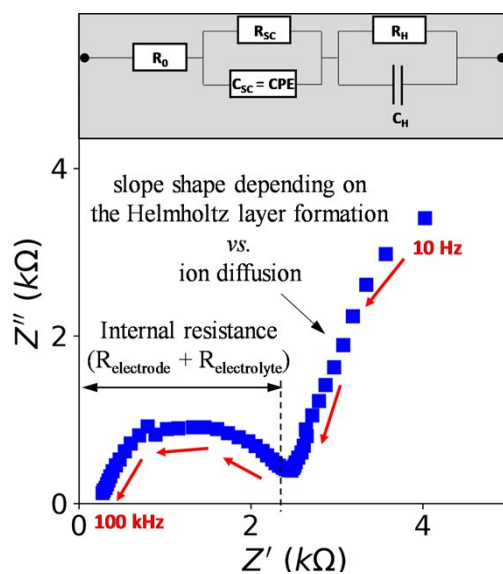


Figure SI-3: Nyquist plot obtained on sample S1 for $V_0 = 1.6$ V vs. RHE. The equivalent electric circuit used in the fitting procedure is shown. The slope at intermediate frequencies, indicated by the black arrow, is a measure of the Helmholtz layer extent

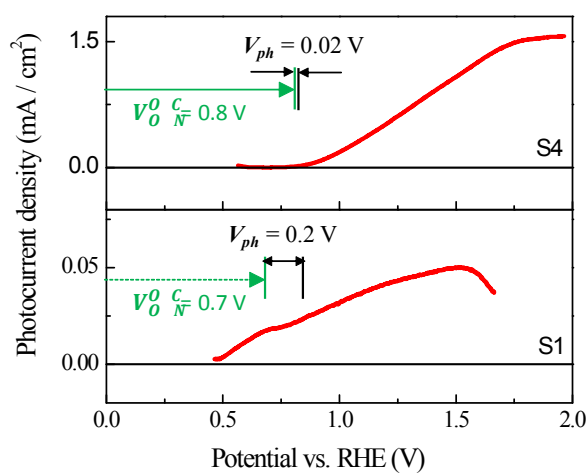


Figure SI-4: Open circuit potential values obtained with and without light on samples S1 and S4. Higher photovoltage values are obtained on pure hematite sample (S1). The onset potential is equal to V_{ON}^{OC}

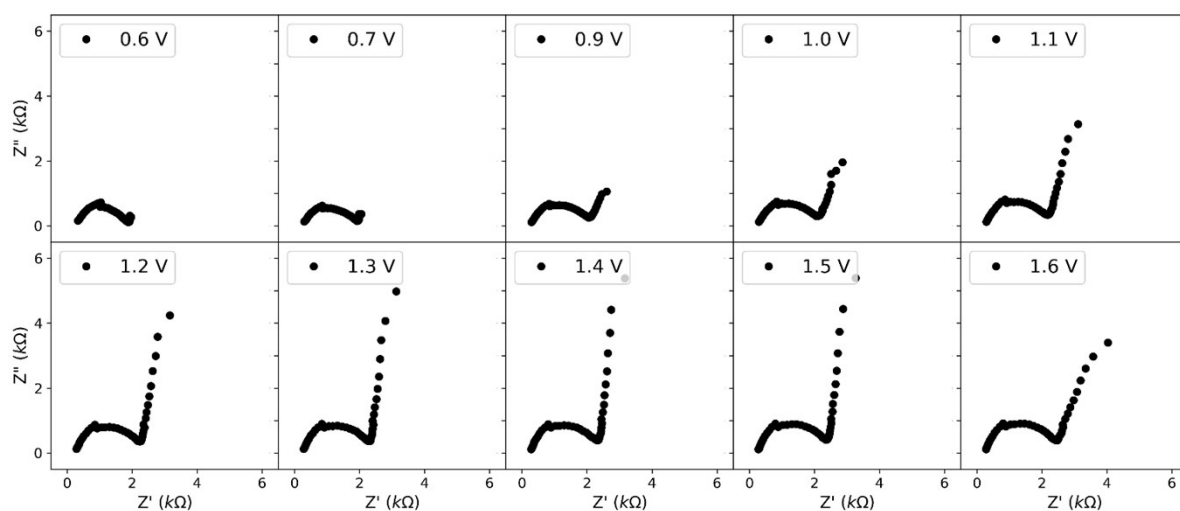


Figure SI-5: The evolution of the slope on the Nyquist plots corresponding to the double layer formation vs. ion diffusion obtained on sample S1 for different values of the anodic potential between

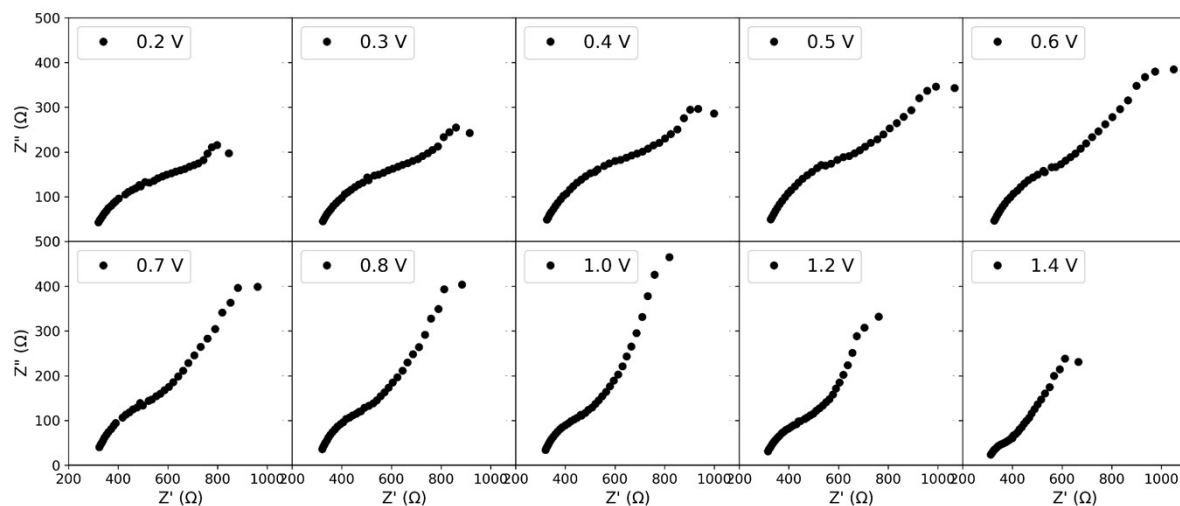


Figure SI-6 : The evolution of the slope on the Nyquist plots corresponding to the double layer formation vs. ion diffusion obtained on sample S4 for different values of the anodic potential between 0.2V and 1.4 V vs. RHE

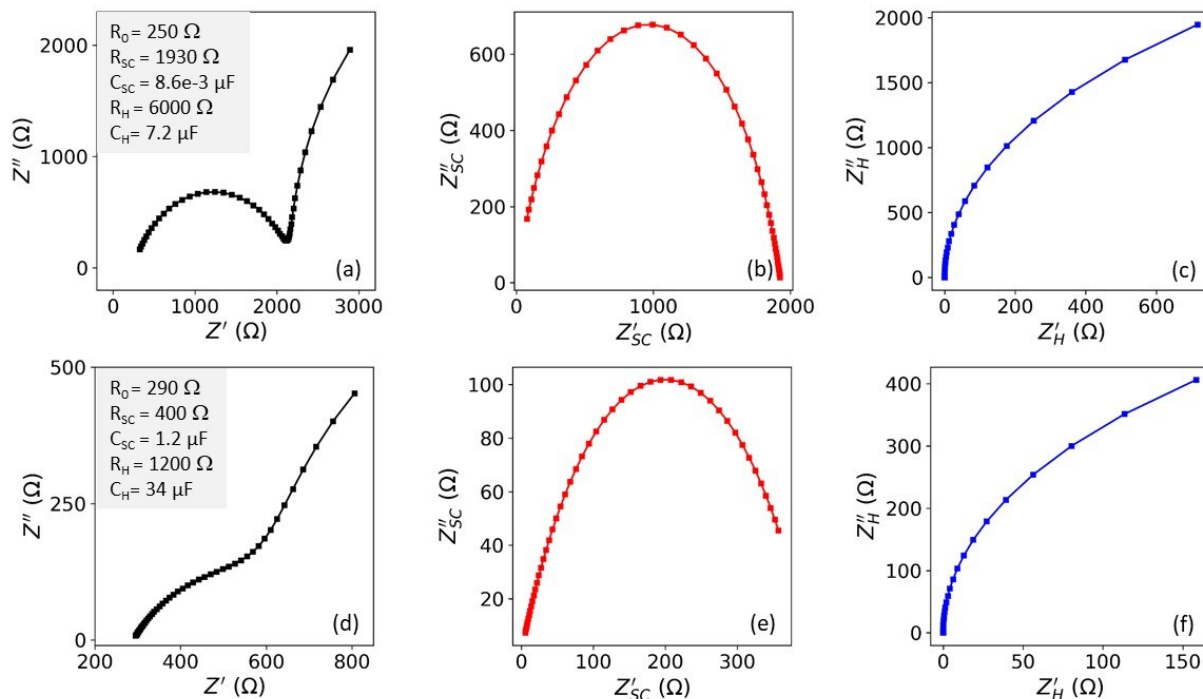


Figure SI-7 : a) Modeled Nyquist plots for high impedance semiconductor in contact with the electrolyte; b) semiconductor and c) Helmholtz contributions to the Nyquist plot; d) Modeled Nyquist plots for low impedance semiconductor in contact with the electrolyte; e) semiconductor and f) Helmholtz contributions to the Nyquist plot. Impedance values used for the modelization correspond to the fit values obtained for pure hematite sample, S1 (high impedance) and Ti-substituted hematite sample, S4 (low impedance).

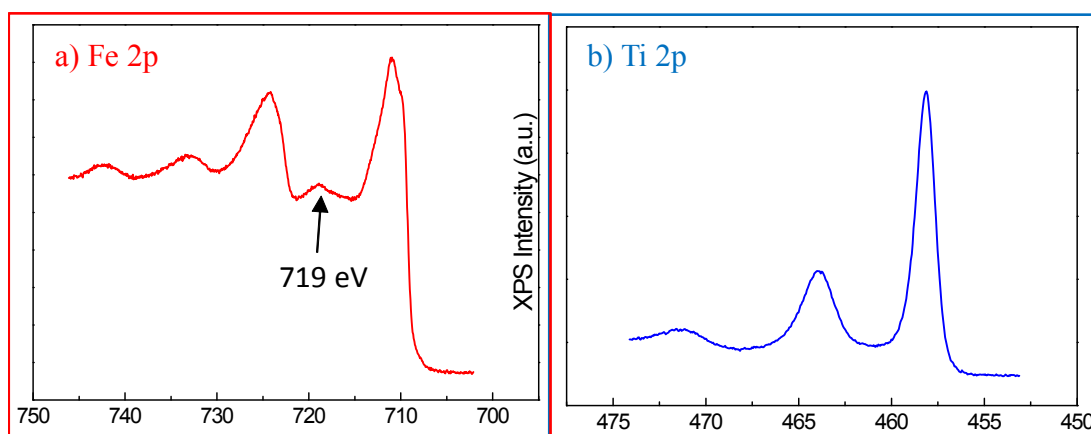


Figure SI-8: Fe2p (a) and Ti2p (b) XPS core level spectra recorded on sample S4. The shake-up peak recorded at 719 eV binding energy is typical for Fe³⁺. Ti spectra show a very narrow peak at 458.1 eV indicating the absence of Ti³⁺ valence states.

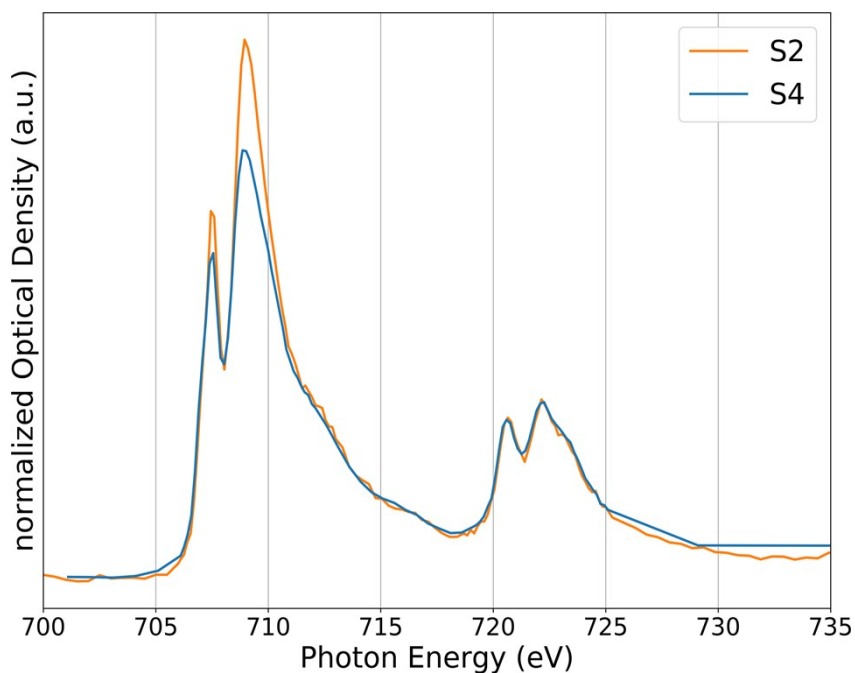


Figure SI-9: Fe L_{2,3} absorption edges recorded for the S2 and S4 samples respectively. The spectrum corresponding to the S4 sample is partly absorption saturated, as indicated by a reduced L₃/L₂ branching ratio, due to the reduced X-ray attenuation length of ~120 nm at the L₃ peak energies. The spectrum of the S2 sample is typical for Fe³⁺ ions in an octahedral coordination, as expected for hematite.

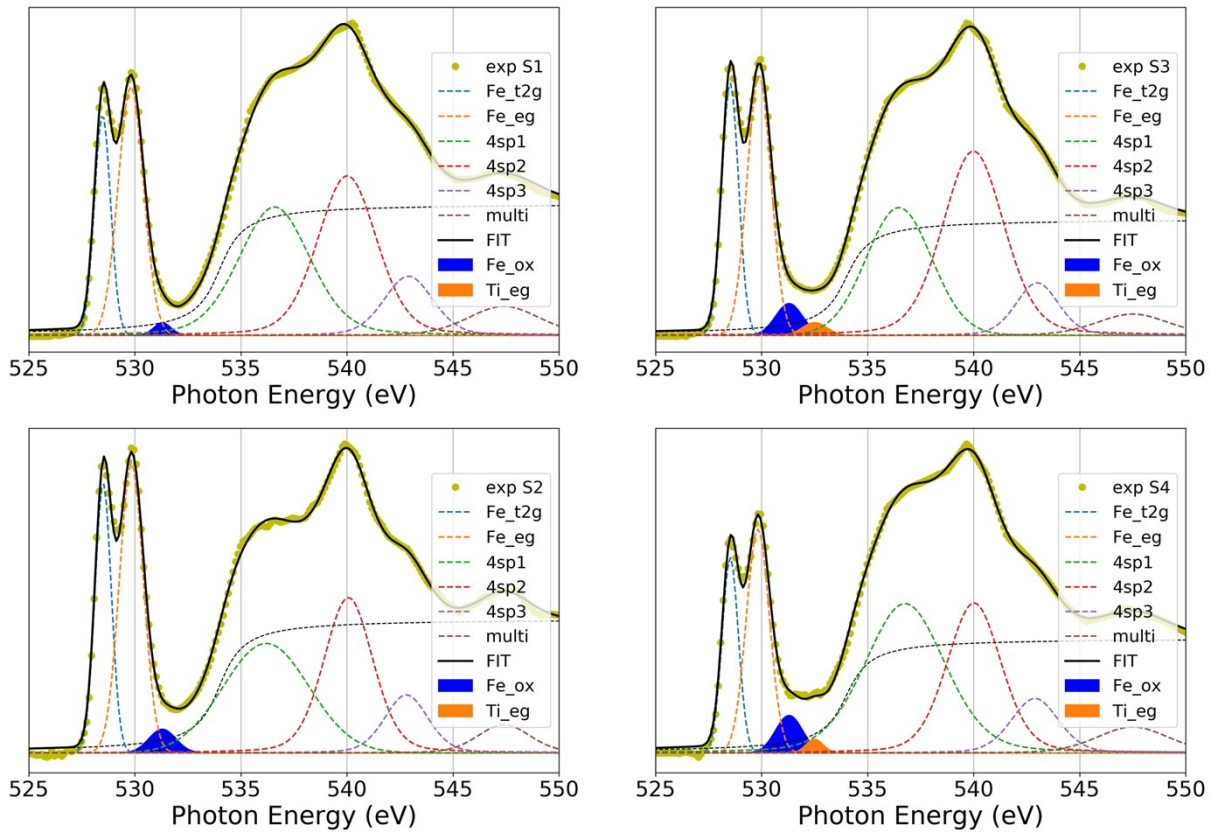


Figure SI-10: Fit of the O K edge absorption spectra for the whole set of samples studied, S1 to S4. We remark the increase of the blue peak corresponding to the oxidative states denoted as Fe-ox upon increasing the annealing temperature from 500 °C to 600 °C. The same arctangent background was used in all cases and the 3 peaks corresponding to the 4sp bands were kept at the same positions and with the same FWHM, only the amplitude was set as free parameter.

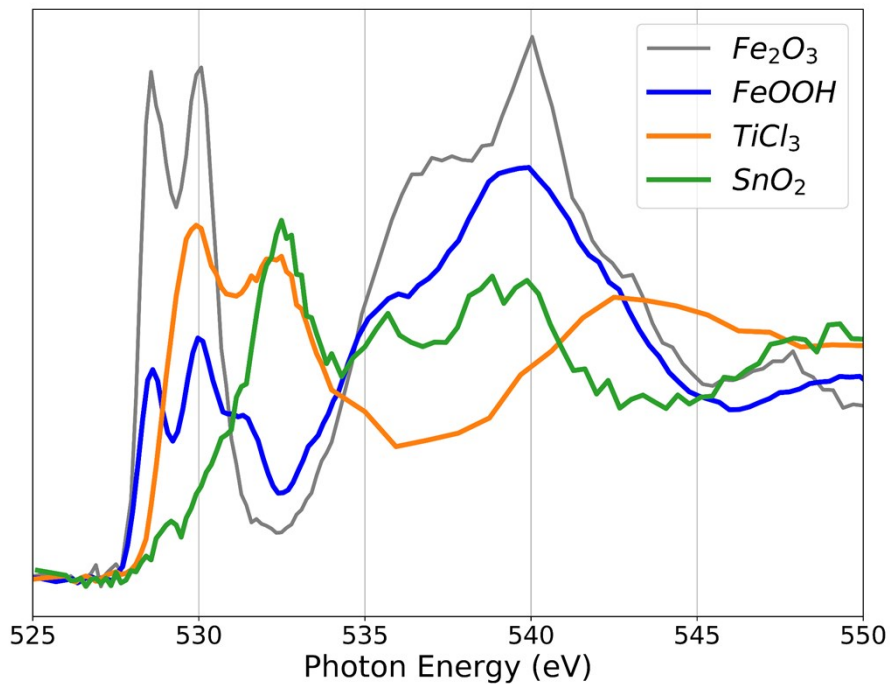


Figure SI-11: Various O K-edge XAS spectral features expected in our samples: hematite (gray), akaganeite (blue), showing the strong OH 1s to O 2p transition at 531.35eV; oxidized TiCl_3 (orange) showing t_{2g} transition overlapping with hematite e_g one; and fluorinated SnO_2 (FTO showing the Sn 5p resonance overlapping with the Ti e_g at 532.5 eV.